ANALYSIS OF ADAPTIVE ARRAY ALGORITHM PERFORMANCE FOR SATELLITE INTERFERENCE CANCELLATION IN RADIO ASTRONOMY

Lisha Li and Brian D. Jeffs

Brigham Young University, Department of Electrical and Computer Engineering
459 CB, Provo, UT 84602, USA, email: bjeffs@ee.byu.edu

ABSTRACT

In this paper we evaluate suitability of several array processing methods for adaptively canceling interfering signals present in radio astronomy. The issue of signal corruption by orbital satellite downlink signals, such as from GLONASS and IRIDIUM, is addressed. Simulation and real data analysis of the achievable SINR improvement and beam mainlobe distortion for five candidate algorithms is presented. Performance is evaluated as a function of angular separation between the signal of interest and the interferer, in the presence of array grating lobes.

1. INTRODUCTION

This paper presents a comparative analysis of several candidate adaptive cancellation array processing algorithms as applied to radio astronomy. These algorithms are well known in the digital signal processing community, but their effectiveness when applied to radio astronomy has not been fully established. We are particularly interested in canceling interference from orbital satellite downlink signals such as from GLONASS and IRIDIUM. These interferers affect critical observation spectral bands used in radio astronomy [1, 2]. For example, GLONASS operates in the important hydroxyl ion (OH) emission band. Satellite interferers can be more problematical than ground-based sources because they are not in fixed locations, and can rapidly traverse both the mainlobe and sidelobes of the telescope beam. This non–stationary interference requires an adaptive processing approach for effective mitigation. The ultimate goal of our work is to use real-time digital signal processors (DSPs) to deal with the time varying nature of signals from satellites in transit.

The particular needs of astronomical observation constitute an extremely demanding environment for array processing algorithms, and it must be determined if these issues can be properly addressed, and which candidate algorithms are best suited. Compared with wireless communications or signal intercept array processing applications, radio astronomy suffers from: 1) extremely low signal to noise ratios, 2) sparse antenna arrays which produce grating lobes, 3) very high gain directional array elements, 4) significant interference appearing in antenna sidelobes where response is not calibrated nor uniform across the array, 5) single antenna high gain telescopes where unmatched smaller auxiliary antennas must be used to form an array, and 6) a need for absolute gain and beam shape calibration to permit accurate science observations (e.g. surface brightness, extent, etc.)

Our research approach is to use a low cost, easily modified test platform of small radio telescopes and real-time digital signal processing to permit rapid development and analysis of interference mitigation algorithms. An array (which we call the BYU Very Small Array, 'VSA') of three 10 foot diameter telescopes has been installed on a rooftop at Brigham Young University. Once an adaptive technique has been vetted on this platform, we will then evaluate its performance on NRAO telescopes with our partners at Green Bank Observatory.

The analysis presented below evaluates some of these issues using mostly simulated data for our three–antenna VSA system. This data accurately models satellite signal properties, including bandwidths, motion, and signal levels, and permits us to evaluate specific scenarios that would be difficult to reproduce with real observed data. A real data example of GLONASS interference excision is also presented.

2. THE ALGORITHMS

This section defines the adaptive algorithms that have been analyzed to evaluate cancellation performance and main beam distortion levels. As others have noted, use of multichannel arrays opens up some powerful spatial filtering options for interference mitigation [3, 1]. Algorithms evaluated to-date include the Linearly Constrained Minimum Variance (LCMV) beamformer, Generalized Sidelobe Canceller (GSC), Multiple Sidelobe Canceller (MSC), Maximum Signal to Noise

This project is supported by National Science Foundation grant number AST-9987339.

Ratio (MSNR) beamformer, and beamforming after Subspace Projection Spatial Nulling (SPSN). Detailed algorithm descriptions can be found in [4, 5, 6, 3]. The following table summarizes how beamformer weights are computed for each method. In all cases, beamformer output is formed as $\mathbf{y}[n] = \mathbf{w}^H \mathbf{x}[n]$, where ^{H} indicates complex conjugate transpose.

Algorithm	Optimization Criterion	Array Weight Solution	Comments
LCMV	$\min_{\mathbf{w}} \mathbf{w}^H \mathbf{R}_{xx} \mathbf{w}$, s.t. $\mathbf{C}^H \mathbf{w} = \mathbf{f}^H$	$\mathbf{w} = \mathbf{f}^H \frac{\mathbf{R}_{xx}^{-1}\mathbf{C}}{\mathbf{C}^H \mathbf{R}_{xx}^{-1} \mathbf{C}}$	$\mathbf{C}$ contains constraint array response vectors. $\mathbf{f}$ is desired response values
GSC	$\min_{\mathbf{w}} [\mathbf{w}_o - \mathbf{C}_n \mathbf{w}]^H \mathbf{R}_{\mathbf{xx}} [\mathbf{w}_o - \mathbf{C}_n \mathbf{w}]$	$\mathbf{w} = \mathbf{w}_o - \mathbf{C}_n \mathbf{w}_n$, $\mathbf{w}_n = \frac{\mathbf{C}_n{}^H \mathbf{R}_{\mathbf{xx}} \mathbf{w}_o}{\mathbf{C}_n{}^H \mathbf{R}_{\mathbf{xx}} \mathbf{C}_n}$	$\mathbf{C}$ & $\mathbf{f}$ as in LCMV. $\mathbf{C}_n = \text{Null}\{\mathbf{C}\}$. $\mathbf{w}_o = \mathbf{C}(\mathbf{C}^H \mathbf{C})^{-1} \mathbf{f}$.
MSC	$\min_{\mathbf{W}_a} E\{\lvert \mathbf{x}_m - \mathbf{W}_a^H \mathbf{x}_a \rvert^2\}$	$\mathbf{w} = \begin{bmatrix} \mathbf{I} \\ \mathbf{W}_a \end{bmatrix} \mathbf{w}_m$ $\mathbf{W}_a = \mathbf{R}_{aa}^{-1} \mathbf{R}_{am}$	$\mathbf{x}[n] = \left[\mathbf{x}_m^T[n],\ \mathbf{x}_a^T[n]\right]^T$, $\mathbf{w}_m$ is any conventional weight to steer main sub array to source.
MSNR	$\max_{\mathbf{w}} \frac{\mathbf{w}^H \mathbf{R}_{ss} \mathbf{w}}{\mathbf{w}^H (\mathbf{R}_{ii} + \mathbf{R}_{\eta\eta}) \mathbf{w}}$	$\lambda_{\max} \mathbf{w} = (\mathbf{R}_{ii} + \mathbf{R}_{\eta\eta})^{-1} \mathbf{R}_{ss} \mathbf{w}$	$\mathbf{R}_{xx} = \mathbf{R}_{ss} + \mathbf{R}_{ii} + \mathbf{R}_{\eta\eta}$ i.e. signal + interference, + noise.
SPSN	$\mathbf{w} \in \text{Null}\{\mathbf{R}_{ii}\}$	$\mathbf{w} = P_i^{\perp} \mathbf{w}_o$ $P_i^{\perp} = \mathbf{I} - \mathbf{U}_i \mathbf{U}_i^{\dagger}$	$\mathbf{U}_i$ = eigenvectors of $\mathbf{R}_{xx}$ corresponding to p largest eigenvalues.

$\mathbf{R}_{xx} = E\{\mathbf{x}[n]\mathbf{x}^H[n]\}$ is the full array covariance matrix. Subscripts $_{aa}$ and $_{am}$ indicate the auxiliary subarray, and auxiliary to main subarray cross covariances respectively. In all analysis to follow, a single ($p = 1$) interferer is assumed, and $\mathbf{w}_m$ and $\mathbf{w}_o$ used in MSC and SPSN respectively were uniform amplitude weights steered to the source.

The LCMV and GSC methods place constraints on the beamformer spatial response so signals from the direction of interest are passed with specified gain and phase. Nulls are adaptively formed on interfering signals and noise arriving from directions other than the constraints. The GSC approach is to transform the constrained minimization problem of the LCMV into an unconstrained minimization. Up to $M - 1$ interferers can be cancelled for an M element array, and mechanical tracking of the interferer is not required. Single mainlobe constraints were used in the following analysis.

The MSC uses a main single high gain channel or a main subarray, $\mathbf{x}_m$, and one or more auxiliary channels, $\mathbf{x}_a$, which have high interference to signal ratio. Auxiliary antennas are usually mechanically steered to interference sources. The MSC is well suited for a single high gain radio telescope like the GBT. The real–time lms adaptive filter reported by Barnbaum and Bradley, and the GLONASS cancellation example below are examples of a single auxiliary channel MSC with sequential estimation of $\mathbf{R_a}$ and $\mathbf{r}_{ma}$ [1].

The primary difficulty in applying the MSNR beamformer in a radio astronomy environment is obtaining separate estimates for $\mathbf{R}_{i+\eta} = (\mathbf{R_i} + \mathbf{R}_\eta)$ and $\mathbf{R_s}$. Some assumptions about signal structure must be applied.

The SPSN method estimates the interference subspace from the sample covariance matrix, and then calculates weights corresponding to beams in the orthogonal complement of this subspace. In SPSN, $\mathbf{U}_i^{\dagger} = (\mathbf{U}_i^H \mathbf{U}_i)^{-1} \mathbf{U}_i^H$ and p is the estimated number of interferers.

3. ALGORITHM PERFORMANCE ANALYSIS

Each of the above algorithms was used in Mote Carlo simulation of interference cancellation for our small three antenna VSA system. Synthetic data was generated representing a single GLONASS satellite while observing a weak OH emission source object. Also, a real data sample of GLONASS interference was obtained from the VSA. For the simulated data, a variety of source–interferer geometries and signal levels were used to determine which algorithms performed best in each situation. All covariance matrices and other parameters required by the algorithms were estimated from the simulated observed data. Each experiment used 100,000 samples of data, corresponding to 12.5 ms of integration, with 100 repeated random trials for each resulting plot point presented below.

Interference Attenuation Near Grating Lobes

Radio astronomical interferometric imaging arrays use widely spaced antennas. Even a small tightly packed array of high gain antennas have inter-element spacing of many wavelengths. This unavoidably (even when reduced by randomized placement and highly directional element responses) introduces grating lobes in any beamforming approach to interference cancellation. In this situation, placing a beamformer null in the direction of the interference suppresses the desired signal as well. Algorithm sensitivity to this effect is studied with this experiment for the VSA. We assume the source of interest

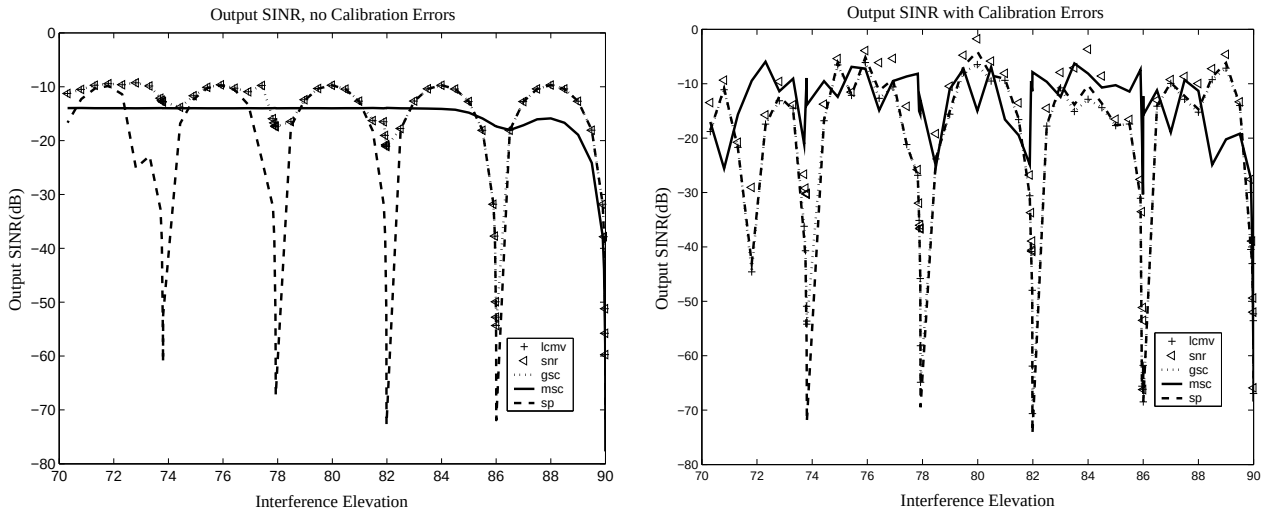

Fig. 1. Adaptive cancellation performance in the presence of grating lobes. Input SINR is -60 dB, with signal 14 dB below noise, and interferer 46 dB above noise. Noise bandwidth is the full 8 Mhz system bandwidth supported by the 8 MHz complex baseband sample rate. Signal and interferer are independent narrowband sources. a) Calibrated array results. Note adaptive cancellation brings the SINR up to approximately the SNR level. b) Performance with multiplicative complex Gaussian random calibration errors, mean of 1.0 and independent real and imaginary variance of 0.01.

comes from zenith, i.e. $0°$ azimuth and $90°$ elevation. We evaluated interference attenuation level achieved by the different algorithms as a function of the elevation of the interference as it approaches zenith while passing through several grating lobes.

Scenarios were evaluated for a variety of signal, noise, and interference power levels, ranging from signal to noise plus interference ratios (SINR) of -120 dB to 0 dB, and signal to noise ratios (SNR) of -20 dB to +48 dB. In all cases, the MSC was far less affected by grating lobes than were the LCMV, GSC, MSNR, and SPSN processors. The LCMV, GSC, and MSNR performed nearly identically, except the GSC suffered a 6 dB to 20 dB drop in cancellation performance when the SNR was high while the SINR was low. These three algorithms and SPSN achieved as much as 100 dB improvement in SINR at the beamformer output, but as expected, provided no improvement when the interferer direction corresponded to a grating lobe. Figure 1 presents the results of two typical scenarios.

Sensitivity to Array Calibration Errors

Array gain and phase calibration errors are inevitable, yet algorithms like LCMV and GSC require accurate calibration information to place the constraints. Our experiments have shown that though realistic calibration errors can affect the interference attenuation level, the total SINR improvement these systems is still acceptable. As shown in Fig. 1b, performance varies markedly among the algorithms in the presence of moderate calibration errors. Still, only the MSC exhibits immunity to grating lobe effects.

Stability of the Main Lobe Shape

A significant concern in astronomical observation is keeping the beam shape consistent so as not to bias scientific measurements. With the LCMV, GSC, and mSNR processors, the beamformer mainlobe shape can be distorted if interference enters at the mainlobe or a grating lobe. This occurs because the algorithm will attempt to place a null on the interferer even if it distorts the beam shape, so long as the output SINR is improved. The simulation results show that when the interference is exactly in a grating lobe, the main lobe shape can be distorted significantly. An example of this is shown in Fig. 2a. However, if the interferer moves off the grating lobe direction a few degrees, the main lobe shape is well maintained and good enhancement of output SINR is achieved.

Real Data GLONASS MSC Experiment

Figure 2b presents results demonstrating GLONASS interference removal from real VSA data using the MSC algorithm. The plot represents a 250 ms integration, 1024 bin power spectrum over an 8 Mhz band. One VSA dish was tracking the

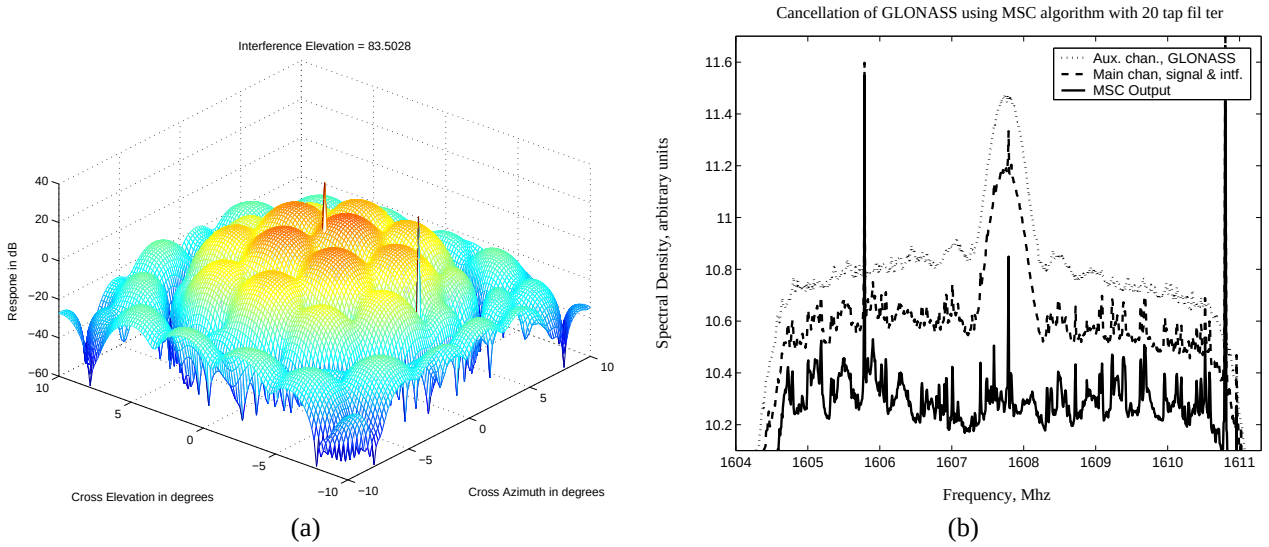

Fig. 2. a) Example of mainbeam distortion for interference within $2.5°$ of a grating lobe. Spikes (left to right) mark source and interference locations. Note the central mainlobe peak is offset from the source direction. b) Real VSA GLONASS data MSC example. Note spectral line riding on main channel GLONASS interference is retained in cancelled MSC output. Large spectral lines to left and right of GLONASS signal are local interference seen in main channel.

satellite as an auxiliary antenna, while the main dish received another signal of interest with GLONASS corruption. In the MSC output the GLONASS signal appears completely removed, while the signal line is preserved. Note that in this recent data, obtained during the first week of VSA operation, the desired signal was a a local ground based interference, and not a true deep-space OH line.

4. CONCLUSIONS

Our early experiments suggest that adaptive array processing algorithms do hold promise for satellite interference excision in radio astronomy. Problems with grating lobe interactions and calibration errors do exist, but are tractable. These methods are particularly attractive when the interference level at the antenna output is many decibels above the signal. In this case the interferer can often be driven down to the background noise level.

5. REFERENCES

[1] C. Barnbaum and R.F. Bradley, "A new approach to interference excision in radio astronomy: Real-time adaptive cancellation," *Astronomical Journal*, vol. 116, pp. 2598–2614, Nov. 1998.

[2] S.W. Ellingson, J.D. Bunton, and J.F. Bell, "Cancellation of glonass signals from radio astronomy data," in *Proceedings of the SPIE, Conference 4015*, Munich, Mar. 2000, pp. 400–407.

[3] A. Leshem, A.J. van der Veen, and A.J. Boonstra, "Multichannel interference mitigation techniques in radio astronomy," *Astrophysical Journal Supplements*, vol. 131, no. 1, pp. 355–374, 2000.

[4] B.D. Van Veen and K. M. Buckley, "Beamforming: A versatile approach to spatial filtering," *IEEE ASSP Magazine*, pp. 4–24, Apr. 1988.

[5] J. Raza, A.-J. Boonstra, and A.-J. van der Veen, "Spatial filtering of rf interference in radio astronomy," *IEEE Signal Processing Letters*, vol. 9, no. 2, pp. 64–67, Feb. 2002.

[6] S.W. Ellingson and G.A. Hampson, "A subspace-tracking approach to interference nulling for phased array-based radio telescopes," *IEEE Transactions on Antennas and Propagation*, vol. 50, no. 1, pp. 25–30, Jan. 2002.